Influence of Different Bandwidths on LAI Estimation Using Vegetation Indices

Liang Liang, Ting Huang, Liping Di, *Senior Member, IEEE*, Di Geng, Juan Yan, Shuguo Wang, Lijuan Wang, Li Li, Bingqian Chen, and Jianrong Kang

***Abstract*—Leaf area index (LAI) is a valuable indicator used in vegetation growth monitoring. To optimize the index selection according to the type of remote sensing data and to improve the inversion accuracy of LAI, this article analyzes the influence of different bandwidths on the accuracy of the inversion model based on vegetation indices. First, the simulation dataset is generated by the PROSAIL model, and on this basis, 15 vegetation indices with high correlation coefficients with LAI. Then, by analyzing the sensitivity of these 15 indices to the variations in bandwidth, and to the coefficient of determination (R^2) of the LAI inversion model with the variations of bandwidth, the influence of different bandwidths on the accuracy of LAI estimation by each index is determined. The results show that bandwidth is one of the most important factors in determining the accuracy of LAI inversion, and the influence on different vegetation indices can be divided into the following three categories. First, narrowband vegetation index, the accuracy of inversion models built by vegetation indices decreases with the increase of bandwidth, including $SR_{[800,680]}$, OSAVI, MTVI2, $SR_{[752,690]}$, RDVI, NDCI, and NVI. Second, middleband vegetation index, the accuracy first increases and then decreases with the increase of bandwidth, including $SR_{[700,670]}$, Carte5, and $SR_{[675,700]}$. Third, broadband vegetation index, the accuracy increases with the increase of bandwidth, including SPVI, Carte2, OSAVI2, MTVI1, and $NDVI_{705}$. The study provides a scientific basis for vegetation index optimization in the process of LAI inversion.**

***Index Terms*—Bandwidth, leaf area index (LAI), PROSAIL model, vegetation index.**

Manuscript received January 16, 2020; revised March 3, 2020; accepted March 24, 2020. Date of publication April 3, 2020; date of current version April 27, 2020. This work was supported in part by the Natural Science Foundation of Jiangsu Province under Grant BK20181474, in part by Xuzhou Key R&D Projects under Grant KC19134, in part by the Open Fund of State Key Laboratory of Remote Sensing Science under Grant OFSLRSS201804, in part by the National Natural Science Foundation of China under Grant 41971305, and in part by the Project Funded by the Priority Academic Program Development of Jiangsu Higher Education Institutions. *(Corresponding authors: Liang Liang; Liping Di.)*

Liang Liang, Ting Huang, Di Geng, Juan Yan, Shuguo Wang, Lijuan Wang, Bingqian Chen, and Jianrong Kang are with the College of Geography Surveying and Urban-Rural Planning, Jiangsu Normal University, Xuzhou 221000, China (e-mail: liang_rs@jsnu.edu.cn; lllxwjhht@163.com; 15190665389@163.com; yan_juan2@126.com; swang@jsnu.edu.cn; wanglj2013@jsnu.edu.cn; bingqiancumt@163.com; jrkang@263.net).

Liping Di is with the Center for Spatial Information Science and Systems, George Mason University, Fairfax, VA 22030 USA (e-mail: ldi@gmu.edu).

Li Li is with the State Key Laboratory of Remote Sensing Science, Aerospace Information Research Institute of Chinese Academy of Sciences, Beijing 100101, China (e-mail: lili_1452@163.com).

Digital Object Identifier 10.1109/JSTARS.2020.2984608

I. Introduction

LEAF area index (LAI) is the sum of the area of a single green leaf per unit surface area. It can reflect the physiological and biochemical characteristics of vegetation, and is one of the important structural parameters of vegetation. Remote sensing technology can obtain the spatiotemporal information of LAI at a lower cost than other technologies, and it has become the most common method for obtaining this indicator on a macroscale [1]–[3].

Estimating LAI more accurately from remote sensing data has been one of the hot topics in vegetation remote sensing [4]–[7]. To improve the accuracy and universality of the inversion model, on the one hand, researchers constantly optimize and improve inversion strategies and algorithms to reduce model errors [8]–[10]. On the other hand, they are committed to analyzing the effects of soil background [11], soil type [12], observation geometry [13], hot spot effect [14], and other factors in the inversion process of LAI in order to find corresponding methods to reduce or eliminate the impact of interference factors. Studies have shown that the selection of vegetation index type and bandwidth in calculation are also important factors affecting the inversion of vegetation parameters [15]–[17]. The selection of a vegetation index currently depends only on the previous studies, or else it must be determined by screening various indices, which increases the uncertainty and complexity of inversion process. However, due to the influence of bandwidth, even if the same index is used for LAI inversion, the results are often quite different. For example, when Twele *et al.* used NDVI (normalized difference vegetation index), SR (simple ratio), RSR (reduced simple ratio), NDVIc (corrected normalized difference vegetation index), and SAVI2 (soil adjusted vegetation index 2) to estimate the LAI of the forest canopy, they found that this type of vegetation index can obtain higher inversion accuracy in a narrowband [16]. The inversion research of rice LAI by Wang *et al.* showed that the best results can be obtained when NDVI is calculated using a spectrum with a bandwidth of 15 nm [18]. Due to the different bandwidths of different sensor data, the optimal index can only be selected by exhaustive research methods, a mechanism that is not generally applicable to the actual remote sensing application process [19], [20]. Therefore, the systematic analysis of the impact of the bandwidth on the vegetation indices during LAI inversion is of great significance for improving the accuracy of LAI inversion.

This article will use the PROSAIL canopy simulation dataset to analyze the vegetation indices commonly used in LAI

TABLE I
RANGE OF INPUT PARAMETERS FOR PROSAIL5B

Parameters	Description	Min	Max	Mean	Variance
N	Leaf structural parameter	1	2	1.5	1
Car (mg/cm^2)	Carotenoid content	6	10	8	2
Cab (mg/cm^2)	Leaf chlorophyll content	10	90	40	20
Cw (cm)	Equivalent water thickness	0.003	0.05	0.015	0.015
Cm (g/cm^2)	Dry matter content	0.002	0.02	0.0075	0.0075
LAI	Leaf area index	0.1	10	2	2.5
ALA	Mean leaf inclination angle	30	80	50	10
hspot	Hot spot parameters	0.05	0.1	0.0075	0.03
psoil	Soil brightness parameters	0.3	0.9	0.7	0.4
tts (°)	Solar zenith angle	0	60	30	30
tto (°)	Observation zenith angle	0	60	30	30
Psi (°)	Observation relative azimuth	0	180	90	90
Skyl	Fraction of diffuse incoming solar radiation	0	40	20	20

inversion and to study the influence of different bandwidths on LAI inversion accuracy, so as to provide the basis for determining the optimal bandwidth of vegetation index in theory and selecting vegetation indices in real-world remote sensing applications (i.e., to select the appropriate vegetation index for different sources of remote sensing data).

II. DATA AND METHODS

A. PROSAIL Spectral Datasets

The PROSAIL radiative transfer model combines the PROSPECT leaf optical properties model [21] and the SAIL canopy bidirectional reflectance model [22], which gives it the advantages of simplicity, accuracy, and availability. It can describe the reflection characteristics of the uniform vegetation canopy and has been widely used in the inversion of biophysical and biochemical parameters. The number and distribution of input parameters in the PROSAIL model will affect the inversion results of LAI. The parameter range of the leaf dataset used in this article is shown in Table I and all the parameters involved in the simulation of the canopy spectral data set adhere to the Gaussian normal distribution. Discrete parameters are generated according to the predefined discrete levels, and then the discrete parameters are completely arranged and combined using an orthogonal experiment design to generate 15 000 parameter data sets. Then, 15 000 simulated canopy spectra can be obtained by inputting 15 000 parameter data groups into the PROSAIL model. The simulation of PROSAIL spectral data set is generated by MATLAB software. The input parameters of the model are as follows: N, Car, Cab, Cw, Cm, LAI, ALA, hspot, psoil, tts, tto, Psi, Skyl. Table I shows the specific parameter settings. The wavelength of simulated canopy spectra generated by PROSAIL 5B[1] ranges from 450 to 2500 nm, increasing in 1 nm steps [23].

[1]http://teledetection.ipgp.jussieu.fr/prosail/

TABLE II
SELECTED VEGETATION INDICES

Vegetation Index	Expression	References
$SR_{[800,680]}$	R_{800}/R_{680}	[24]
OSAVI	$(1+0.16)(R_{800}-R_{670})/(R_{800}+R_{670}+0.16)$	[25]
MTVI2	$\frac{1.5[1.2(R_{800}-R_{550})-2.5(R_{670}-R_{550})]}{\sqrt{(2R_{800}+1)^2-(6R_{800}-5\sqrt{670})-0.5}}$	[26]
NDCI	$(R_{762}-R_{527})/(R_{762}+R_{527})$	[27]
$SR_{[700,670]}$	R_{700}/R_{670}	[28]
SPVI2	$0.4*3.7(R_{800}-R_{670})-1.2\lvert R_{550}-R_{670}\rvert$	[29]
Carte2	R_{695}/R_{760}	[30]
NVI	$(R_{777}-R_{747})/R_{673}$	[31]
SPVI	$0.4*3.7(R_{800}-R_{670})-1.2\lvert R_{530}-R_{670}\rvert$	[32]
OSAVI2	$(1+0.16)(R_{750}-R_{705})/(R_{750}+R_{705}+0.$	[33]
$SR_{[675,700]}$	R_{675}/R_{700}	[34]
Carte3	R_{605}/R_{760}	[30]
MTVI1	$1.2[1.2(R_{800}-R_{550})-2.5(R_{670}-R_{550})]$	[26]
RDVI	$(R_{800}-R_{670})/\sqrt{R_{800}+R_{670}}$	[35]
$NDVI_{705}$	$(R_{750}-R_{705})/(R_{750}+R_{705})$	[36], [37]
GNDVI	$(R_{750}-R_{550})/(R_{750}+R_{550})$	
TVI	$0.5[120(R_{750}-R_{550})-2.5(R_{670}-R_{550})]$	[38]
RI_{1dB}	R_{735}/R_{720}	[39]
$SR_{[752,690]}$	R_{752}/R_{690}	
$SR_{[750,550]}$	R_{750}/R_{550}	[40]
$SR_{[750,710]}$	R_{750}/R_{710}	
Carte5	R_{695}/R_{670}	[30]
Carte4	R_{710}/R_{760}	
VOG1	R_{740}/R_{720}	
VOG2	$(R_{734}-R_{747})/(R_{715}+R_{726})$	[41]
VOG3	$(R_{734}-R_{747})/(R_{715}+R_{720})$	
$mNDVI_{705}$	$(R_{750}-R_{705})/(R_{750}+R_{705}-2R_{445})$	[42], [24]
Datt2	R_{850}/R_{710}	[30]
mSR_{705}	$(R_{750}-R_{445})/(R_{705}-R_{445})$	[42], [24]
$SR_{[750,700]}$	R_{750}/R_{700}	[43]

B. Construction of the Inversion Model

An empirical inversion method can estimate LAI accurately by establishing a function relationship between LAI and the vegetation index. Based on previous research, 30 vegetation indices published for LAI inversion are primarily selected in this article to study the correlation between vegetation index and LAI under different bandwidths (see Table II). The types of indices included simple ratio indices (e.g., $SR_{[800,680]}$), normalized difference ratios (e.g., $NDVI_{705}$), triangular vegetation indices (e.g., TVI), and modified versions of these three types of indices (e.g., MTVI1). In the modeling, the vegetation index was used as the independent variable x, and the LAI of the PROSAIL model was used as the dependent variable y. The curve fitting models of vegetation index and LAI are established by using linear regression, exponential regression, logarithmic regression, polynomial regression, and power function regression. Root mean square error (RMSE) and the coefficient of determination (R^2) serve as the evaluation indicators in order to select the optimal model.

C. Extension of Bandwidth

In order to study the influence of bandwidth on the accuracy of LAI inversion, it is necessary to obtain the vegetation index calculated by canopy reflectance at different bandwidths.

In this article, the vegetation canopy spectral reflectivity at different bandwidths is simulated according to formula 1 and formula 2. When expanding the bandwidth, this study sets the initial bandwidth of the canopy spectrum at 5 nm, gradually increases that bandwidth to 80 nm in steps of 5 nm, and then calculates the vegetation index under different bandwidths. The wavelength involved in the calculation of the vegetation index is set as the center wavelength when the bandwidth is expanded. Such a multibandwidth setting not only ensures the richness and continuity of the bandwidth, but also simulates the spectral channel width of most remote sensing satellite sensors, which helps determine the best vegetation index when retrieving the LAI with different satellite sensor data, so as to improve the precision of the LAI inversion. The specific formula is [17]

$$\rho_j = \int_{\lambda_s(j)}^{\lambda_e(j)} \rho(\lambda) S_j(\lambda) d\lambda \Big/ \int_{\lambda_s(j)}^{\lambda_e(j)} S_j(\lambda) d\lambda \quad (1)$$

where ρ_j is the leaf reflectance of the simulated band j, $\rho(\lambda)$ is the simulated spectral reflectance of the PROSAIL model, and $\lambda_s(j)$ and $\lambda_e(j)$ are the start and end wavelengths of band j, respectively. $S_j(\lambda)$ is the spectral response function of band j. In this article, the Gaussian function is used to simulate the spectral response function of the remote sensing satellite sensors. The specific formula is

$$S_j(\lambda) = \exp - \left(\frac{\lambda - c_j}{\mathrm{FWHM}_k / \left(2\sqrt{ln2}\right)} \right)^2 \quad (2)$$

where c_j is the center wavelength of band j, and FWHM_k is the expanded bandwidth (5, 10, …, 80 nm).

D. Sensitivity of Vegetation Index to LAI and Bandwidth

In order to quantitatively compare and evaluate the sensitivity of the vegetation index to the bandwidth, the vegetation index calculated at expanding the bandwidth is compared with that calculated at the original bandwidth (1 nm). The Var_{bw} (sensitivity coefficient of bandwidth) is defined as follows [17]:

$$Var_{\mathrm{bw}} = \frac{|(VI_{i,j} - VI_{1,j})|_{\max}}{VI_{\max}} \quad (3)$$

where i is bandwidth (5, 10, …, 80 nm), j is LAI, and $VI_{i,j} - VI_{1,j}$ is the difference between the vegetation index of bandwidth i and the vegetation index of bandwidth 1 nm when LAI is the same. When Var_{bw} is larger, it means that the vegetation index is more sensitive to the bandwidth.

At the same time, a quantitative analysis of the sensitivity of the vegetation reflectance spectrum to physical and chemical parameters is the premise of remote sensing inversion [44]. In order to quantitatively describe the sensitivity of spectral indices to LAI, the degree of change of Var_{LAI} (the sensitivity coefficient of LAI) [16] with changing LAI values was calculated according to the formula given as follows:

$$Var_{\mathrm{LAI}} = \frac{(|VI|_{\max} - |VI|_{\min})}{VI_{\max}} \quad (4)$$

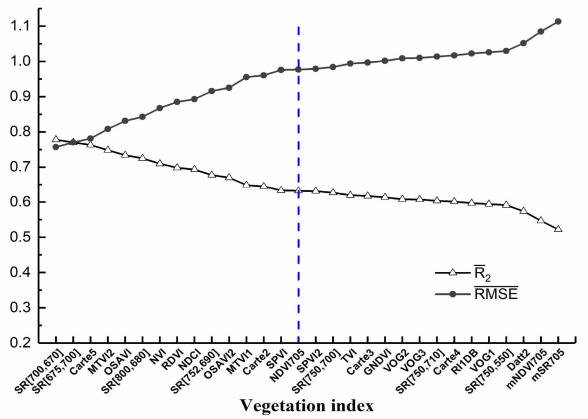

Fig. 1. Accuracy of the best fitting model of vegetation indices.

where VI represents the vegetation index calculated in this article, and $VI_{\max}$ and $VI_{\min}$ represent the maximum and minimum values of the vegetation index with the variation of LAI, respectively.

III. Results and Analysis

A. Modeling and Selection of Vegetation Index

The best curve fitting models of vegetation indices differ. In order to evaluate the capability of different vegetation indices to retrieve LAI, the best fitting models of each vegetation index are selected for curve fitting. First, the R^2 and RMSE of the LAI model established by each vegetation index when the bandwidth is between 5 and 80 nm were calculated. Based on the result, the $\overline{R^2}$ (mean value of coefficient of determination) and $\overline{\mathrm{RMSE}}$ (mean value of RMSE) were calculated to better evaluate the comprehensive estimation ability of vegetation indices at different bandwidths. The results are shown in Fig. 1. In general, the higher the accuracy of the LAI estimation model, the larger the R^2 and the smaller the RMSE are. In this article, $\overline{R^2}$ and $\overline{\mathrm{RMSE}}$ were used as precision evaluation indices to screen the vegetation index. The vegetation index with $\overline{R^2}$ in the top 50% was selected, and the selected vegetation indices are $\mathrm{SR}_{[700,670]}$, $\mathrm{SR}_{[675,700]}$, Carte5, MTVI2, OSAVI, $\mathrm{SR}_{[800,680]}$, NVI, RDVI, NDCI, $\mathrm{SR}_{[752,690]}$, OSAVI2, MTVI1, Carte2, SPVI, and NDVI_{705}, which have the potential to accurately estimate LAI.

B. Sensitivity Analysis of Vegetation Index

Fig. 2 shows the sensitivity coefficient of the selected 15 vegetation indices to bandwidth. It can be seen that the Var_{bw} of the vegetation index was basically positively related to the bandwidth, and the larger Var_{bw} was, the lower the interference resistance of the vegetation index to the bandwidth. The above results show that bandwidth is one of the most important factors affecting the vegetation index, and as the bandwidth increases, it results in more disturbance of the vegetation index selected in this article.

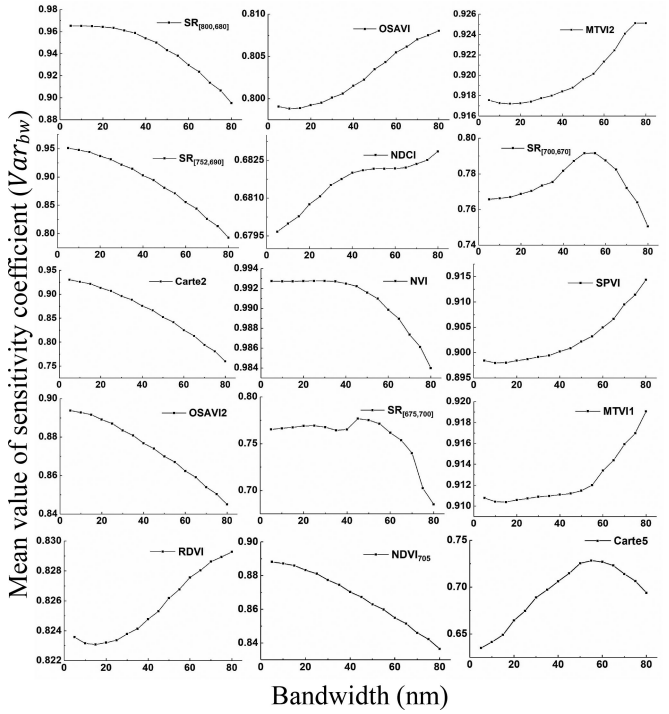

Fig. 2. Sensitivity of vegetation index to bandwidth at different bandwidths.

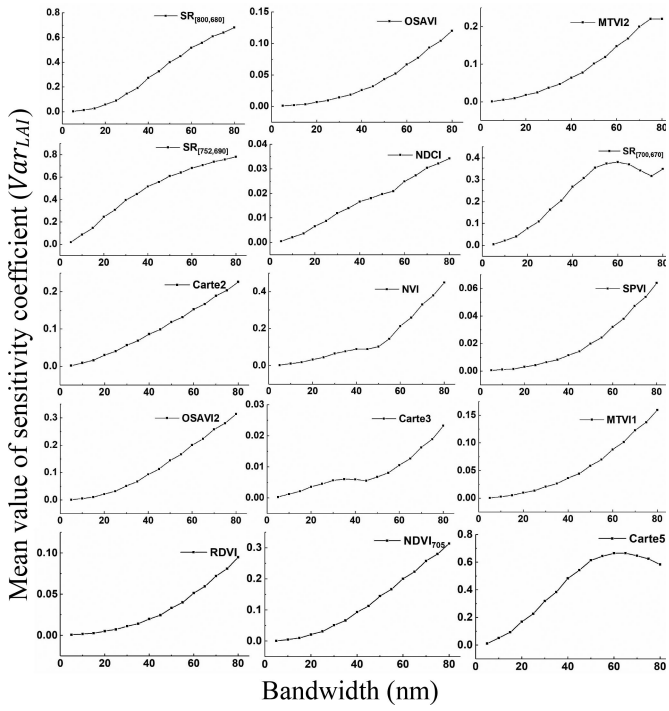

Fig. 3. Sensitivity of vegetation index to LAI at different bandwidths.

The sensitivity coefficient Var_{LAI} calculations are shown in Fig. 3, which represents the sensitivity of the vegetation index to the LAI. It can be seen that the sensitivity coefficient of indices MTVI2, OSAVI, RDVI, NDCI, MTVI1, and MTVI2 was positively correlated with the bandwidth. In contrast, Var_{LAI} of $\mathrm{SR}_{[800,680]}$, $\mathrm{SR}_{[752,690]}$, Carte2, NVI, OSAVI2, and NDVI_{705}

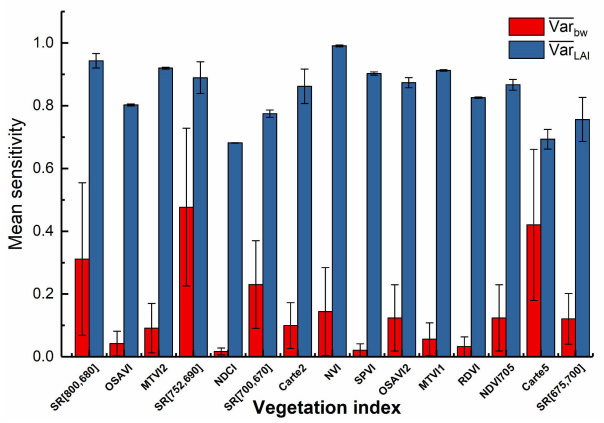

Fig. 4. Mean value of sensitivity coefficients.

showed a decreasing correlation with the increase of bandwidth. However, the sensitivity coefficient curves of Carte5, $\mathrm{SR}_{[700,670]}$, and $\mathrm{SR}_{[675,700]}$, had significant peaks between 5 and 80 nm.

This shows that bandwidth will also change the response of the vegetation index to LAI. Therefore, based on the preliminary analysis of the variation of Var_{bw} and Var_{LAI} with the bandwidth, it can be inferred that bandwidth is an important factor affecting the accuracy of LAI estimation, and the influence of bandwidth on the accuracy of LAI estimation by different vegetation indices may differ as well. However, the specific impact of bandwidth on LAI estimation using a vegetation index still requires further study and analysis.

At the same time, in order to compare the sensitivity of each vegetation index to the bandwidth more intuitively, the $\overline{Var_{\mathrm{LAI}}}$ (mean value of Var_{LAI}) and $\overline{Var_{\mathrm{bw}}}$ (mean value of Var_{bw}) were calculated when the bandwidth was 5 to 80 nm, as shown in Fig. 4. It can be seen that the 15 vegetation indices selected in this article were all affected by the bandwidth. Among them, $\overline{Var_{\mathrm{bw}}}$ of NDCI, SPVI, and RDVI were smaller and less affected by the bandwidth, so they had good stability. However, $\mathrm{SR}_{[752,690]}$, Carte5, $\mathrm{SR}_{[800,680]}$, $\mathrm{R}_{[700,670]}$ were more susceptible to the influence of bandwidth. Meanwhile, It can be seen that MTVI2, MTVI1 are not only highly sensitive to the changes in LAI, but also have good anti-interference to the bandwidth. In contrast, the vegetation indices Carte5 and $\mathrm{SR}_{[700,670]}$ have high sensitivity to the bandwidth and low response to LAI. After preliminary analysis, the LAI estimation models constructed by MTVI2 and MTVI1 may have better performance.

The spectral reflectance generated by the simulated spectral response function was used to calculate the value of 15 vegetation indices at bandwidths between 5 and 80 nm, and the correlation between the vegetation index and LAI was then studied. Fig. 5 shows the change in the vegetation index with the increase of LAI. Each vegetation index shows a different degree of saturation when LAI increases. Most vegetation indices gradually became more saturated when LAI > 1. This type of vegetation index is more suitable for the estimation of low-value LAI. For example, the indices OSAVI, NDCI,

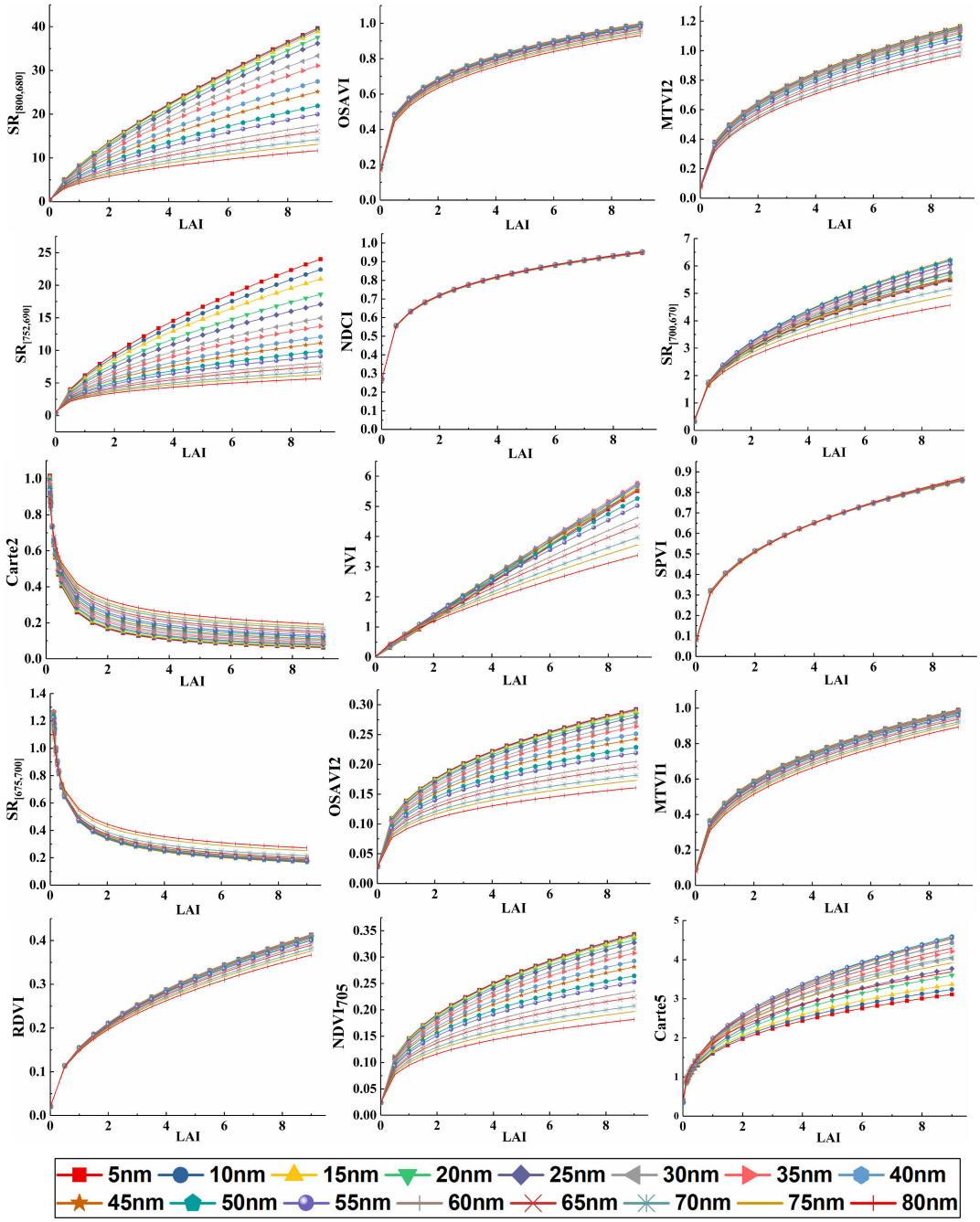

Fig. 5. Changes of 15 vegetation indices on LAI increase.

Carte2, and $SR_{[675,700]}$ increased or decreased rapidly when LAI < 1, but obviously reached saturation when LAI > 1, indicating that this type of index is more suitable for LAI inversion of sparse canopy. The saturation state of NVI was not obvious, indicating that the index is sensitive to changes in LAI and may be suited for the estimation of LAI. The vegetation index and the LAI are mainly logarithmic and power-correlated, among which $SR_{[675,700]}$, Carte2, and LAI are negatively related.

It is worth noting that the correlation between LAI and vegetation index calculated by spectral reflectance at different bandwidths can vary dramatically. As the bandwidth increases, Carte5 becomes more sensitive to the change of LAI, while $SR_{[700,670]}$, $SR_{[675,700]}$, MTVI2, OSAVI, $SR_{[800,680]}$, NVI, RDVI, $SR_{[752,690]}$, OSAVI2, MTVI1, Carte2, and $NDVI_{705}$ are less sensitive to LAI as the bandwidth increases. The influence of the bandwidth on SPVI and NDCI is small, and the change with the increase of LAI at each bandwidth is basically nonexistent, which corresponds to the above research results (that is, the calculated $\overline{Var_{\mathrm{bw}}}$ of SPVI and NDCI is smaller). Therefore, the vegetation index and bandwidth selected for our calculations are important factors affecting the inversion of vegetation parameters.

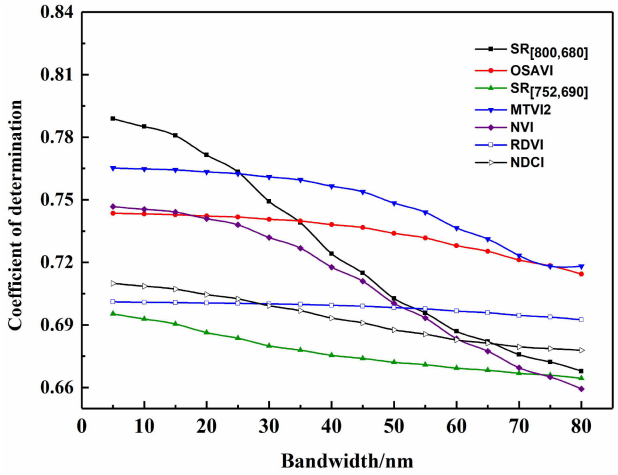

Fig. 6. R^2 of LAI estimation model for narrowband vegetation indices at different bandwidths.

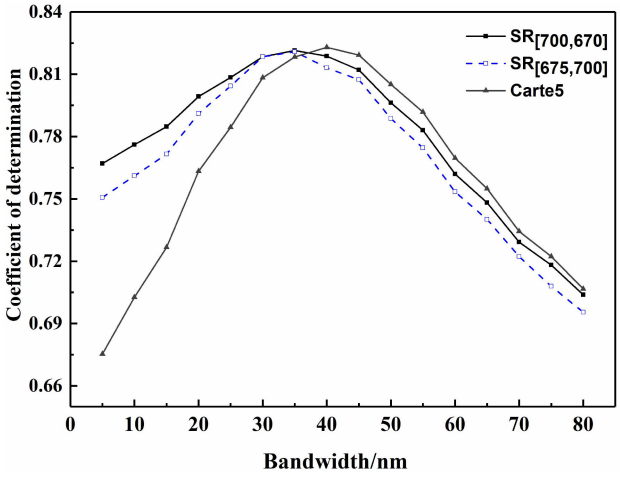

Fig. 7. R^2 of LAI estimation model for middleband vegetation indices at different bandwidths.

C. Inversion Accuracy of LAI Varies With Bandwidth

Figs. 6–8 show the R^2 of the LAI inversion model built by different indices, changing with the bandwidth. According to the change trend of R^2, each index can be divided into the following three categories.

1) The R^2 of inversion model decreases continuously with the increase of the bandwidth, that is, the narrower the band, the more appropriate it is. These types of indices can be called narrowband indices.
2) R^2 first rises and then falls with the increase of bandwidth, and the curve has an obvious peak value, which can be called the middleband index.
3) R^2 increases with the increase of bandwidth, that is, in the analysis range of this article (bandwidth $\leq$ 80 nm), the wider the band is, the more appropriate it is. This can be called the broadband index.

Fig. 6 shows that the R^2 of LAI estimation model built by narrowband vegetation indices ($SR_{[800,680]}$, OSAVI, MTVI2, $SR_{[752,690]}$, RDVI, NDCI, and NVI) varies with different bandwidths. It can be seen that with the increase of the bandwidth, the model R^2 built by the narrowband vegetation index is basically unchanged, and they all show a downward trend. Fig. 6 shows that the narrower the bandwidth, the better the ability of the model constructed by this type of index to estimate LAI. Therefore, when using hyperspectral remote sensing data to estimate LAI, narrowband vegetation indices should be given priority in order to obtain better estimation results. In addition, when the bandwidth is less than 25 nm, R^2 of LAI inversion model built by index $SR_{[800,680]}$ is the highest, followed by MTVI2, OSAVI, and NVI. Therefore, these four indices can be used as the optimal indices for LAI inversion with hyperspectral data (the spectral channel range is generally less than 10 nm). However, $SR_{[800,680]}$ and NVI decrease sharply with the increase of the bandwidth, which indicates that the LAI inversion model constructed by these two indices is extremely susceptible to the bandwidth. When using different remote sensing data sources to estimate LAI, the results may differ significantly. Therefore, combining the sensitivity analysis of vegetation indices and the results of R^2 changing with bandwidth, MTVI2 and OSVAI can be determined as the optimal indices for LAI hyperspectral inversion.

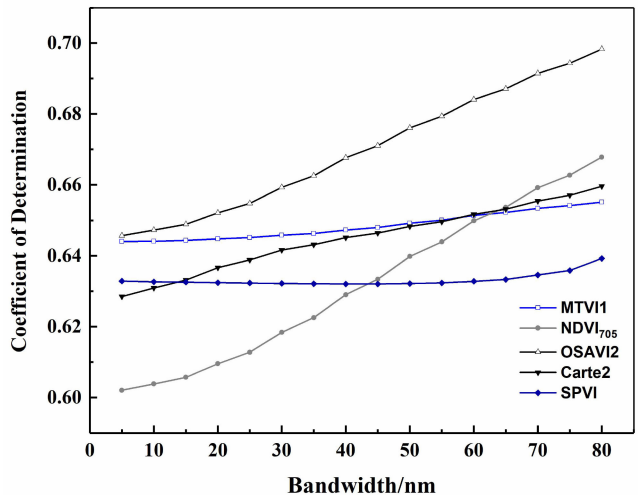

Fig. 8. R^2 of LAI estimation model for broadband vegetation indices at different bandwidths.

Fig. 7 shows that the R^2 of LAI estimation models built by middleband vegetation indices ($SR_{[700,670]}$, Carte5, and $SR_{[675,700]}$) varies with different bandwidths. The characteristic of this type of index is that when the bandwidth is less than 30 nm, the R^2 of the model increases with the broadening of the bandwidth and decreases when the peak value appears at a bandwidth of 30 to 45 nm. The optimal bandwidth of $SR_{[700,670]}$ and $SR_{[675,700]}$ is about 35 nm, and that of Carte5 is 40 nm. When using remote sensing to retrieve LAI, remote sensing data with high spectral resolution is often difficult to obtain due to limited conditions. Therefore, the middleband vegetation index has significant application potential in the LAI inversion process. At the same time, by combining the $\overline{R^2}$ of the vegetation indices analyzed above, we determine

that the middleband vegetation indices, particularly the LAI estimation models built by $SR_{[700,670]}$ and $SR_{[675,700]}$, achieve precise estimation results under 60 nm, and that both are more suitable for hyperspectral/medium spectral resolution remote sensing data (particularly suitable for remote sensing data with a spectral channel width of about 35–40 nm). Therefore, in order to obtain high-precision estimation results of LAI when using hyperspectral/medium spectral resolution remote sensing data to estimate canopy LAI, it is best to try to select the middleband vegetation indices.

Fig. 8 shows that the R^2 of the LAI estimation model built by broadband vegetation indices (SPVI, Carte2, OSAVI2, MTVI1, and $NDVI_{705}$) varies with different bandwidths. The significant feature of the broadband vegetation indices is that the R^2 of its LAI inversion model has a positive correlation with LAI, indicating that the larger the bandwidth, the better the estimation ability of the model. At the same time, it can be seen from the figure that the R^2 of OSAVI2 is always the highest, which shows that the ability of OSAVI2 to estimate LAI is better than other broadband vegetation indices, but also shows that the change curve of R^2 of model built by SPVI and MTVI1 is relatively smooth, and that the ability to retrieve LAI is stable. It is worth noting that the R^2 of model built by the broadband vegetation indices is always smaller than that of the narrowband vegetation indices and the middleband vegetation indices, and has certain advantages only when the bandwidth is greater than 35 nm.

IV. Discussion

The results of the research above show that bandwidth is an important factor in LAI estimation by vegetation indices, and different vegetation indices have their optimal bandwidths for inversion. By analyzing the variation of R^2 with bandwidth, it is found that the estimation accuracy of $SR_{[800,680]}$, $SR_{[752,690]}$, and NVI at wide bandwidth is much lower than that at narrow bandwidth. According to the knowledge of spectroscopy, narrower bandwidth can obtain more sensitive information, while wide bandwidth can make full use of the information of a certain spectral region. Therefore, the inversion accuracy of narrowband vegetation index such as $SR_{[800,680]}$, mainly depends on whether the sensitive band can be accurately located, while for broadband index such as SPVI, the improvement of inversion accuracy depends more on whether the information of the spectral region is fully utilized. In recent years, more studies on LAI estimation using vegetation indices from hyperspectral data [45]–[49] have been carried out, and better inversion results have been achieved due to the optimization of vegetation indices from narrowband spectral data [50]. However, hyperspectral remote sensing sensors (narrowband) need to collect large amounts of data in a short time, which often leads to complex technical problems, and may also have a low signal-to-noise ratio [51]. Therefore, it is still necessary to find some vegetation indices suitable for broadband to take part in the inversion of physical and chemical parameters. This study shows that the optimal bandwidth for $SR_{[700,670]}$, Carte5, and $SR_{[675,700]}$ to estimate LAI is between 55 and 60 nm, while the broadband vegetation indices studied in this article have a higher accuracy in estimating LAI at a wideband. Therefore, during the estimation of LAI, the determination of the optimal bandwidth of vegetation indices provides a certain reference for the selection of the appropriate vegetation indices according to remote sensing data with different spectral resolutions.

At the same time, most of the current studies compare the ability of different vegetation indices to retrieve LAI at a single bandwidth [52]–[53]. However, the influence of each bandwidth on the vegetation indices differs. For example, when the bandwidth is less than 60 nm, the model estimation accuracy of OSAVI2 is significantly better than that of MTVI1, but when the bandwidth is greater than 60 nm, the result is the opposite. This shows that it is of limited use to evaluate the ability of an index to estimate vegetation parameters only according to the inversion accuracy of the vegetation index at a certain bandwidth. Therefore, in this experiment, we evaluated 30 vegetation indices to retrieve LAI at bandwidths of 5 to 80 nm, which not only ensured the variety of the vegetation indices but also the continuity of bandwidth.

V. Conclusion

In this article, we analyzed the sensitivity of different vegetation indices to LAI and bandwidth, as well as the influence of bandwidth on the accuracy of the model when these indices are used to estimate LAI. On this basis, we determined the optimal bandwidth of LAI retrieved by various vegetation indices. We came to the following three main conclusions.

1) Bandwidth is one of the most important factors affecting the accuracy of LAI inversion. The analysis in this article shows that the accuracy of the inversion model is not only related to the type of vegetation index, but also to the bandwidth used to calculate the index.
2) The influence of bandwidth on the three types of vegetation indices (narrowband, middleband, and broadband) is quite different. With the narrowband vegetation index, the accuracy of the inversion model decreases continuously as the bandwidth increases. This type of index includes $SR_{[800,680]}$, OSAVI, MTVI2, $SR_{[752,690]}$, RDVI, NDCI, and NVI. With the middleband vegetation index, which mainly includes $SR_{[700,670]}$, Carte5, and $SR_{[675,700]}$, the accuracy of the model first increases and then decreases with the increase of the bandwidth. Their best bandwidth is 35 nm, 40 nm, and 35 nm, respectively. With the broadband vegetation index, the accuracy of the model increases with the broadening of the bandwidth. This type includes the indices SPVI, Carte2, OSAVI2, MTVI1, and $NDVI_{705}$.
3) The research results in this article indicate that when using a vegetation index to retrieve LAI, the channel width and spectral resolution of the remote sensing satellite sensor should be considered in order to select the optimal vegetation index. The narrowband vegetation indices are more suitable for hyperspectral remote sensing data, while middleband or broadband vegetation indices are more suitable for multispectral remote sensing data.

REFERENCES

[1] L. Liang *et al.*, "Estimation of crop LAI using hyperspectral vegetation indices and a hybrid inversion method," *Remote Sens. Environ.*, vol. 165, no. 8, pp. 123–134, Aug. 2015.

[2] O. Mutanga, A. K. Skidmore, and H. H. T. Prins, "Predicting in situ pasture quality in the Kruger National Park, South Africa, using continuum-removed absorption features," *Remote Sens. Environ.*, vol. 89, no. 3, pp. 393–408, Feb. 2004.

[3] H. Fang, "Retrieving leaf area index using a genetic algorithm with a canopy radiative transfer model," *Remote Sens. Environ.*, vol. 85, no. 3, pp. 257–270, May 2003.

[4] Y. Q. Liu *et al.*, "Comparing the performance of broad-band and narrow-band vegetation indices for estimation of grass LAI," *Remote Sens. Technol. Appl.*, vol. 29, no. 4, pp. 587–593, Aug. 2014.

[5] M. Y. Shu *et al.*, "High spectral inversion of winter wheat LAI based on new vegetation index," *Sci. China-Chem.*, vol. 51. no. 18, pp. 3486–3496, Sep. 2018.

[6] Z. Liu *et al.*, "Retrieval rice leaf area index using random forest algorithm based on GF-1 WFV remote sensing data," *Remote Sens. Technol. Appl.*, vol. 33, no. 3, pp. 458–464, Jun. 2018.

[7] P. P. J. Roosjen *et al.*, "Improved estimation of leaf area index and leaf chlorophyll content of a potato crop using multi-angle spectral data – potential of unmanned aerial vehicle imagery," *Int. J. Appl. Earth. Observ. Geoinf.*, vol. 66, pp. 14–26, Apr. 2018.

[8] S. Tang *et al.*, "LAI inversion algorithm based on directional reflectance kernels," *J. Environ. Manage.*, vol. 83, no. 3, pp. 638–648, Nov. 2007.

[9] G. Leonenko, S. O. LOS, and P. R. J. North, "Retrieval of leaf area index from MODIS surface reflectance by model inversion using different minimization criteria," *Remote Sens. Environ.*, vol. 139, pp. 257–270, Dec. 2013.

[10] W. Woodgate *et al.*, "An improved theoretical model of canopy gap probability for Leaf Area Index estimation in woody ecosystems," *Forest. Ecol. Manage.*, vol. 358, pp. 303–320, Dec. 2015.

[11] A. R. Huete *et al.*, "A soil-adjusted vegetation index (SAVI)," *Remote Sens. Environ.*, vol. 25, no. 3, pp. 295–309, Aug. 1988.

[12] L. GAO *et al.*, "Exploring the influence of soil types underneath the canopy in winter wheat leaf area index remote estimating," *Chin. J. Plant. Ecol*, vol. 41, no. 12, pp. 1273–1288, Dec. 2017.

[13] G. J. Yang *et al.*, "Inversion of forest leaf area index calculated from multi-source and multi-angle remote sensing data," *Chin. Bull. Botany*, vol. 45, no. 5, pp. 566–578, Sep. 2010.

[14] J. Zhao *et al.*, "Inversion of LAI by considering the hotspot effect for different geometrical wheat," *Spectrosc. Spectral Anal.*, vol. 1, pp. 207–211, Jan. 2014.

[15] D. Zhao *et al.*, "A comparative analysis of broadband and narrowband derived vegetation indices in predicting LAI and CCD of a cotton canopy," *ISPRS J. Photogramm.*, vol. 62, no. 1, pp. 25–33, May 2007.

[16] A. Twele, S. Erasmi, and M. Kappasa, "Spatially explicit estimation of leaf area index using EO-1 hyperion and landsat ETM+ data: Implications of spectral bandwidth and shortwave infrared data on prediction accuracy in a tropical montane environment," *GISCI Remote Sens.*, vol. 45, no. 2, pp. 229–248, Apr. 2008.

[17] H. Du *et al.*, "Evaluation of spectral scale effects in estimation of vegetation leaf area index using spectral indices methods," *Chin. Geogr. Sci.*, vol. 26, no. 6, pp. 731–744, Dec. 2016.

[18] F. M. Wang *et al.*, "Estimation of rice LAI by using NDVI at different spectral bandwidths," *Chin. J. Appl. Ecol.*, vol. 18, no. 11, pp. 2444–2450, Nov. 2007.

[19] L. Liang *et al.*, "Estimation of leaf nitrogen content in wheat using new hyperspectral indices and a random forest regression algorithm," *Remote Sens.*, vol. 10, no. 12, pp. 1940–1956, Dec. 2018.

[20] L. Liang *et al.*, "Estimating crop chlorophyll content with hyperspectral vegetation indices and the hybrid inversion method," *Int. J. Remote. Sens.*, vol. 37, no. 13/14, pp. 2923–2949, Jun. 2016.

[21] S. Jacquemoud and F. Baret, "PROSPECT: A model of leaf optical properties spectra," *Remote Sens. Environ.*, vol. 34, no. 2, pp. 75–91, Nov. 1990.

[22] W. Verhoef, "Light scattering by leaf layers with application to canopy reflectance modeling: The SAIL model," *Remote Sens. Environ.*, vol. 16, no. 2, pp. 125–141, Oct. 1984.

[23] J. B. Feret *et al.*, "PROSPECT-4 and 5: Advances in the leaf optical properties model separating photo-synthetic pigments," *Remote Sens. Environ.*, vol. 112, no. 6, pp. 3330–3043, Jun. 2008.

[24] D. A. Sims and J. A. Gamon, "Relationships between leaf pigment content and spectral reflectance across a wide range of species, leaf structures and developmental stages," *Remote Sens. Environ.*, vol. 81, no. 2, pp. 337–354, Aug. 2002.

[25] G. Rondeaux, M. Steven, and F. Baret, "Optimization of soil-adjusted vegetation indices," *Remote Sens. Environ.*, vol. 55, no. 2, pp. 95–107, Feb. 1996.

[26] D. Haboudane *et al.*, "Hyperspectral vegetation indices and novel algorithms for predicting green LAI of crop canopies: Modeling and validation in the context of precision agriculture," *Remote Sens. Environ.*, vol. 90, no. 3, pp. 337–352, Apr. 2004.

[27] A. Marshak *et al.*, "Cloud-vegetation interaction: Use of normalized difference cloud index for estimation of cloud optical thickness," *Geophys. Res. Lett*., vol. 27, no. 12, pp. 1695–1698, Feb. 2000.

[28] J. E. McMurtrey III *et al.*, "Distinguishing nitrogen fertilization levels in field corn (Zea mays L.) with actively induced fluorescence and passive reflectance measurements," *Remote Sens. Environ.*, vol. 47, no. 1, pp. 36–44, Jan. 1994.

[29] M. Vincini, E. Frazzi, and P. D'Alessio, "Angular dependence of maize and sugar beet VIs from directional CHRIS/PROBA data," in *Proc. 4th ESA CHRIS PROBA Workshop*, 2006, pp. 19–2.

[30] G. A. Carter, "Ratios of leaf reflectance in narrow wavebands as indicators of plant stress," *Int. J. Remote. Sens.*, vol. 15, no. 3, pp. 697–703, Feb. 1994.

[31] R. K. Gupta, D. Vijayan, and T. S. Prasad, "New hyperspectral vegetation characterization parameters," *Adv. Space. Res.*, vol. 28, pp. 201–206, Dec. 2001.

[32] R. Main *et al.*, "An investigation into robust spectral indices for leaf chlorophyll estimation," *ISPRS J. Photogramm.*, vol. 66, no. 6, pp. 751–761, Aug. 2011.

[33] C. Wu *et al.*, "Estimating chlorophyll content from hyperspectral vegetation indices: Modeling and validation," *Agricultural Forest Meteorol.*, vol. 148, no. 8, pp. 1230–1241, Jul. 2008.

[34] E. W. Chappelle, M. S. Kim, and M. M. Iii, "Ratio analysis of reflectance spectra (RARS): An algorithm for the remote estimation of the concentrations of chlorophyll A, chlorophyll B, and carotenoids in soybean leaves," *Remote Sens. Environ.*, vol. 39, no. 3, pp. 239–247, Mar. 1992.

[35] J. L. Roujean and F. M. Breon, "Estimating PAR absorbed by vegetation from bidirectional reflectance measurements," *Remote Sens. Environ.*, vol. 51, no. 3, pp. 375–384, Mar. 1995.

[36] A. Gitelson and M. N. Merzlyak, "Quantitative estimation of chlorophyll-A using reflectance spectra: Experiments with autumn chestnut and maple leaves," *J. Photochem. Photobiol. B*, vol. 22, no. 3, pp. 247–252, Mar. 1994.

[37] A. Gitelson and M. N. Merzlyak, "Spectral reflectance changes associated with autumn senescence of *Aesculus hippocastanum* L. and *Acer platanoides* L. leaves. Spectral features and relation to chlorophyll estimation," *J. Plant Physiol.*, vol. 143, no. 2, pp. 286–292, 1994.

[38] N. H. Broge and E. Leblanc, "Comparing prediction power and stability of broadband and hyperspectral vegetation indices for estimation of green leaf area index and canopy chlorophyll density," *Remote Sens. Environ.*, vol. 76, no. 2, pp. 156–172, May 2001.

[39] R. K. Gupta, D. Vijayan, and T. S. Prasad, "Comparative analysis of red-edge hyperspectral indices," *Adv. Space. Res.*, vol. 32, no. 11, pp. 2217–2222, Dec. 2003.

[40] P. J. Zarco-Tejada and J. R. Miller, "Land cover mapping at BOREAS using red edge spectral parameters from CASI imagery," *J. Geophys. Res.*, vol. 104, no. D22, pp. 27921–27933, 1999,

[41] J. E. Vogelmann, B. N. Rock, and D. M. Moss, "Red edge spectral measurements from sugar maple leaves," *Int. J. Remote Sens.*, vol. 14, pp. 1563–1575, 1993.

[42] B. Datt, "A New reflectance index for remote sensing of chlorophyll content in higher plants: Tests using Eucalyptus leaves," *J. Plant. Physiol.*, vol. 154, no. 1, pp. 30–36, Jan. 1999.

[43] A. A. Gitelson and M. N. Merzlyak, "Remote estimation of chlorophyll content in higher plant leaves," *Int. J. Remote Sens.*, vol. 18, no. 12, pp. 2691–2697, 1997.

[44] Y. F. Xiao *et al.*, "Sensitivity of canopy reflectance to biochemical and biophysical variables," *J. Remote Sens.*, vol. 2015, no. 3, pp. 368–374, May 2015.

[45] D. Haboudane, "Hyperspectral vegetation indices and novel algorithms for predicting green LAI of crop canopies: Modeling and validation in the context of precision agriculture," *Remote Sens. Environ.*, vol. 90, no. 3, pp. 337–352, Dec. 2004.

[46] J. Delegido *et al.*, "Retrieval of chlorophyll content and LAI of crops using hyperspectral techniques: Application to PROBA/CHRIS data," *Int. J. Remote Sens.*, vol. 29, no. 24, pp. 7107–7127, Dec. 2008.

[47] R. Darvishzadeh *et al.*, "Leaf area index derivation from hyper- spectral vegetation indices and the red edge position," *Int. J. Remote Sens.*, vol. 30, no. 23, pp. 6199–6218, Jan. 2009.
[48] S. T. Brantley, J. C. Zinnert, and D. R. Young, "Application of hyperspectral vegetation indices to detect variations in high leaf area index temperate shrub thicket canopies," *Remote Sens. Environ.*, vol. 115, no. 2, pp. 514–523, Feb. 2011.
[49] D. Mairaj *et al.*, "Evaluating hyperspectral vegetation indices for leaf area index estimation of *Oryza sativa* L. at diverse phenological stages," *Front. Plant Sci.*, vol. 8, pp. 1–17, May 2017.
[50] P. S. Thenkabail, R. B. Smith, and E. D. Pauw, "Hyperspectral vegetation indices and their relationships with agricultural crop characteristics," *Remote Sens. Environ.*, vol. 71, no. 2, pp. 158–182, Feb. 2000.
[51] P. S. Thenkabail *et al.*, "Accuracy assessments of hyperspectral waveband performance for vegetation analysis applications," *Remote Sens. Environ.*, vol. 91, no. 3/4, pp. 354–376, Jun. 2004.
[52] A. C. Xavier and C. A. Vettorazzi, "Mapping leaf area index through spectral vegetation indices in a subtropical watershed," *Int. J. Remote Sens.*, vol. 25, no. 9, pp. 1661–1672, May 2004.
[53] Z. Li and X. Guo, "A suitable vegetation index for quantifying temporal variation of leaf area index (LAI) in semiarid mixed grassland," *Can. J. Remote Sens.*, vol. 36, no. 6, pp. 709–721, Jan. 2010.

Liang Liang received the Ph.D. degree in photogrammetry and remote sensing from the Central South University, Changsha, China, in 2010.

He is currently an Associate Professor with Jiangsu Normal University, Xuzhou, China. He has been engaged in remote sensing research for more than 10 years and has authored or coauthored more than 60 publications. His current research is mainly on vegetation parameter inversion and NPP estimation based on remote sensing data and its applications in agriculture and environment.

Ting Huang received the bachelor's degree in 2017 from the School of Geography, Geomatics and Planning, Jiangsu Normal University, Xuzhou, China, where she is currently working toward the master's degree in photogrammetry and remote sensing.

Her research interests include quantitative remote sensing of vegetation and ecological remote sensing.

Liping Di (Senior Member, IEEE) received the Ph.D. degree in remote sensing/GIS (geography) from the University of Nebraska-Lincoln, Lincoln, NE, USA, in 1991.

He is currently a Professor and a Founding Director with the Center for Spatial Information Science and Systems, George Mason University. He has been engaged in geoinformatics research for more than 30 years, authored and coauthored more than 450 publications, and received more than $55 million research grants. His current research is mainly on geoinformatics and its applications in agriculture and environment.

Di Geng received the bachelor's degree in 2018 from the School of Geography, Geomatics and Planning, Jiangsu Normal University, Xuzhou, China, where she is currently working toward the master's degree in photogrammetry and remote sensing.

Her research interests include carbon sink model research and urban carbon sink research.

Juan Yan received the bachelor's degree from the School of Surveying and Mapping and Geographical Sciences, LiaoNing Technical University, LiaoNing, China, in 2015. She is currently working toward the master's degree in photogrammetry and remote sensing with Jiangsu Normal University, Xuzhou, China.

Her research interests include factors influencing the precision of vegetation physical and chemical parameters inversion.

Shuguo Wang received the B.S. degree in photogrammetry and remote sensing from Wuhan University, Wuhan, China, in 2003, and the Ph.D. degree in cartography and geography information system from the Graduate University of Chinese Academy of Sciences, Beijing, China, in 2010.

From 2011 to 2014, he was with the Cold and Arid Regions Environmental and Engineering Research Institute, Chinese Academy of Sciences, Lanzhou, China. Since 2014, he has been with the School of Geography, Geomatics and Planning, Jiangsu Normal University, Xuzhou, China. His research interests include microwave remote sensing, estimation of soil moisture by multisource observation data, and related validation issues.

Lijuan Wang received the Ph.D. degree in cartography and geographical information system from the Chinese Academy of Sciences, Beijing, China, in 2013.

She is currently a Lecturer with Jiangsu Normal University, Xuzhou, China. Her research interests include quantitative remote sensing, agriculture, ecology remote sensing, etc.

Li Li received the B.Sc. degree in geographic information system from Jilin University, Changchun, China, in 2002, the M.Sc. degree in cartography and geography information system from Beijing Normal University, China, in 2005, and the Ph.D. degree in cartography and geography information system from the Institute of Remote Sensing Applications, CAS, Beijing, China, in 2010.

Her current research interests include PAR estimation, FPAR inversion based on remote sensing data and its applications in agriculture and environment.

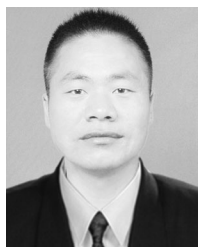

Bingqian Chen received the Ph.D. degree in geodesy and surveying engineering from the China University of Mining and Technology, Xuzhou, China, in 2015.

He is currently an Associate Professor of geodesy with the Jiangsu Normal University, Xuzhou, China. His research focus on radar data processing, deformation monitoring, optimization algorithms, data fusion, and high-performance machine learning approaches for large scale data analysis.

Jianrong Kang received the bachelor's and master's degrees in engineering from Shanxi Mining Institute, Taiyuan, China, in 1988 and 1991, respectively, and the doctor's degree in engineering from the China University of Mining and Technology-Beijing, Beijing, China, in 1999.

He is currently a Professor with the School of Geography, Geomatics and Planning, Jiangsu Normal University, Xuzhou, Jiangsu Province. His research interests include the areas of surveying and mapping engineering, mining subsidence, environmental treatment, and data processing.

Dr. Kang is a member of the Mine Survey Committee and the Mining Damage Technical Appraisal Committee of China Coal Society.